

## A comparative analysis of the microstructural and physicochemical properties of alluvial and dune sands from northeast Algerian Sahara

Article Info:

Article history: Received 2023-06-01 / Accepted 2023-07-20 / Available online 2023-07-25

doi: 10.18540/jcecv19iss6pp16222-01e



**Rafika Hachem**

ORCID: <https://orcid.org/0000-0002-1365-2185>

Department of civil engineering, Faculty of Technology, University of El-Oued, 39000 El-Oued, Algeria

E-mail: [r.hachem@yahoo.fr](mailto:r.hachem@yahoo.fr)

**Nassima Meftah**

ORCID: <https://orcid.org/0000-0001-7646-8572>

Department of Physics, Faculty of Exact Sciences, University of El-Oued, 39000 El-Oued, Algeria

E-mail: [meftahnassima@yahoo.fr](mailto:meftahnassima@yahoo.fr)

**Ahmed Bouaziz**

ORCID: <https://orcid.org/0009-0009-4007-717X>

Civil engineering research laboratory, University of Biskra, Biskra, Algeria

E-mail: [ahmed.bouaziz@univ-biskra.dz](mailto:ahmed.bouaziz@univ-biskra.dz)

### Abstract

This paper investigates the physical, chemical, and microstructural properties of two types of natural sand; alluvial sands and dune sand from the El-Oued region in the northeastern Algerian Sahara. Fourier transform infrared (FTIR) spectroscopy, X-ray diffraction (XRD), X-ray Fluorescence (XRF), Scanning electron microscopy (SEM/EDS), and granulometry analysis have been performed. The FTIR and XRD analysis prove that the alluvial sand and dune sand consist of high percentages of  $\alpha$ -quartz ( $\text{SiO}_2$ ), low amounts of calcite ( $\text{CaCO}_3$ ), and gypsum minerals ( $\text{CaSO}_4 \cdot 2\text{H}_2\text{O}$ ). The chemical analysis confirmed that both types of sand have a high silica ( $\text{SiO}_2$ ) ratio, reaching 80% for dune sand and 70% for alluvial sand, besides very low quantities of  $\text{Al}_2\text{O}_3$ ,  $\text{Fe}_2\text{O}_3$ , and  $\text{K}_2\text{O}$  oxides. CaO content was higher in alluvial sand than in dune sand. The shapes of alluvial sand grain samples ranged from angular to well-rounded. However, the dune sands have shapes ranging from sub-angular to well-rounded. However, the dune sand is poorly graded sand with a mean grain size of  $250\mu\text{m}$ ; whereas, the alluvial sand is well-graded sand with a mean grain size of  $406\mu\text{m}$ . These findings demonstrate that alluvial and dune sands are mineralogically stable and chemically suitable for use as fine aggregates in construction. Also, these sands could be significant sources of quartz minerals.

**Keywords:** Dune sand. alluvial sand. microstructural properties. Construction. X-ray diffraction.

### 1. Introduction

The enormous expansion of industry and infrastructure has caused increases in the consumption of construction materials, particularly natural sand, for various applications. This exploitation has already negatively influenced the ecosystem, causing a water table reduction, an increase in the depth of the river bed, increasing salinity, as well as damaging river embankments (Ayyam *et al.*, 2019; Gourley *et al.*, 2003; Lai *et al.*, 2014; Lollini *et al.*, 2017). Additionally, river sand resources are scarce in many areas, particularly deserts. For these reasons, it became necessary to search for additional and diverse types of high-quality materials for construction projects, and the valorization of local resources became the highest priority (Kirthika *et al.*, 2020).

Dune sand as a construction material is the most attractive due to its properties and low cost, particularly in arid regions where fine natural aggregates are scarce, and dune sands are very abundant (Elipe *et al.*, 2014). Whereas, according to most recommendations and standards for the use of materials in building, dune sand is could be appropriate due to its generally adequate grading size distribution and strong water resistance (Lopez-Querol *et al.*, 2017). Fine aggregate represents approximately one-third of the total amount of concrete aggregates and fills in the gaps. (Ganesan *et al.*, 2022). Fine aggregates are also crucial to preserving the fineness and cohesiveness of concrete (Abu Seif, 2015). The dune sands are unconsolidated sediments formed by the wind's erosion, transportation, and deposition of weathering materials from a sandy parent material in an arid environment (Zhang *et al.*, 2022). They are very distinct granular materials owing to their very uniform particle size distribution, fine mean size, rounded shape of their particles, and very hard to compact without proper lateral confinement (Lopez-Querol *et al.*, 2017). Recently, there has been an emphasis on using aeolian sands as a construction material in concrete, mortar, and pavement. Amri *et al.* (2019) investigated the effects of dune sand treatment upon the geotechnical, structural, as well as mineralogical features of clayey soil. They demonstrated that adding dune sand to clay significantly improves the geotechnical properties. According to Moulay-Ali *et al.*, (2021), the adjusted combination of 20% dune sand, 40% quarry sand, and 60% crushed sand gives the best mechanical resistance to concrete compression. Luo *et al.*, (2013) revealed that the workability as well as durability of concrete incorporating extremely fine dune sand grains from the Australian desert were similar to river sand concrete. Smaida *et al.*, (2019) revealed that dune sand processed using cement, pozzolan, and limestone enhanced the material's mechanical qualities and may be utilized in pavement foundation layers. Accordingly, it is crucial to investigate the physicochemical characterization of dune sand in order to establish its suitability for construction purposes.

Algeria is Africa's largest country, with sand dunes covering nearly a quarter of its surface area. The Algerian Sahara includes one of the world's greatest eolian sand dune deposits (about  $2.4 \cdot 10^6 \text{ km}^2$ ) (Meftah *et al.*, 2021). These sand dunes are divided into ergs, which are vast expanses of continuous sand dunes, with the most significant one being the Grand Oriental Erg (Meftah *et al.*, 2020).

El-Oued City sits in the northeast of Algerian desert. The Grand Erg Oriental covers the majority of this arid region. In contrast, some regions in the northern El-Oued are covered by a mixture of sandy deserts resulting from the disintegration of rocks, with scarce vegetation, scattered oases, and saltwater lakes (Abdelhak *et al.*, 2014). However, the reduction in river sand and the development in demand constitute an irreconcilable conflict due to the long-distance and over-exploitation of river systems. People have experience using the fluvial sand from the north of El-Oued, which results from the disintegration of rocks in construction projects as river sand. Although this sand is used in construction projects in El-Oued, no comprehensive research on its characterization has been found to assess its compliance with standards. Due to the scarcity of this material, the use of dune sand in construction projects has become a necessity due to its availability in huge quantities in this region (Meftah *et al.*, 2021).

In order to assess the appropriateness of El-Oued dune sand for construction, it is necessary to determine its physicochemical characterization in depth. This study presents detailed research about two types of sand: alluvial sand from “El-Baadj region”, which is utilized as construction sand, and dune sands from the El-Oued region. A complete comparative assessment of these two types of sand is presented, including physical properties, sieving analyses, chemical analysis by using non-destructive techniques such as X-ray fluorescence (XRF) and Fourier-transform infrared spectroscopy (FTIR), mineralogical analysis employing X-ray diffraction (XRD), and morphological analysis with Scanning Electron Microscopy with Energy Dispersive Spectroscopy (SEM/EDX).

## 2. Materials and methods

### 2.1 Materials

El-Oued region is a wilaya in the northeastern Algerian Sahara, about 638 km from the capital Algiers; its geographical coordinates are 33°25'0"N and 6°49'60"E (Figure 1). This region is arid, with scorching summers and freezing winters, as well as considerable temperature gradients between night and day (Barkat *et al.*, 2021). As illustrated in Figure 1, sandy dunes are abundant in this area; also, some salt lakes (known as Chotts) in the north of El-Oued city are surrounded by humid sand resulting from the disintegration of rocks. "The Lake of El-Baadj" is one of these lakes where the surrounding sand is used as construction sand.

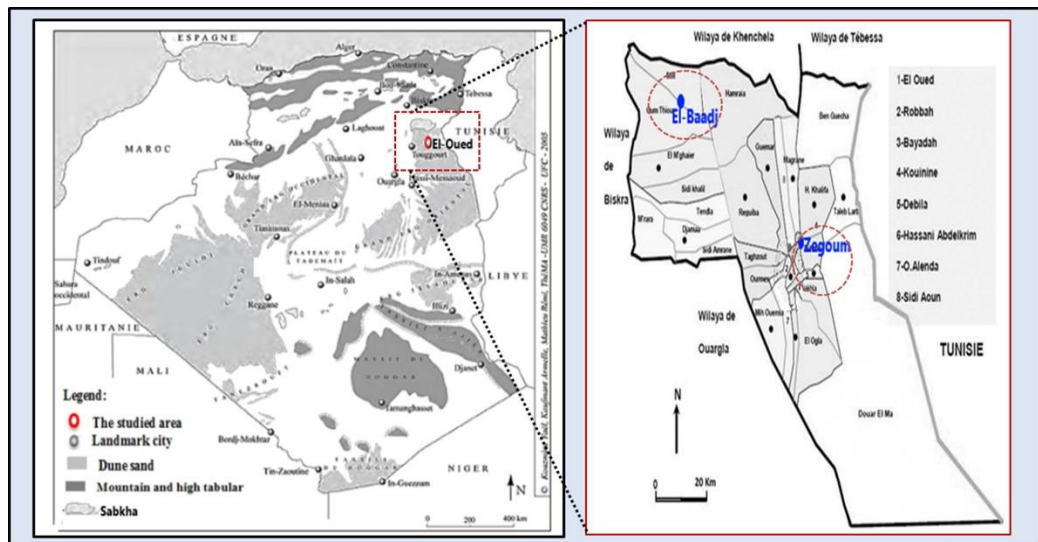


**Figure 1 - The location of the El-Oued region as well as the two investigated sites (Fontaine, 2005).**

For this research, two kind of sand were studied; dune sand and El-Baadj alluvial sand. The dune samples were gathered from numerous dunes in the “Zegoum desert” south of El-Oued city, while the El-Baadj alluvial sand samples were picked up from the “El-Baadj” region in the far northwest of El-Oued province. Equal weights of each sample were combined thoroughly and subsequently dried for 48 hours. After that, various characterizations were established, such as visual examination, physical properties, chemical composition, morphology, and mineral composition. For the latter analysis, the sand samples were manually crushed very well by using a pottery mortar to get a sand powder.

### 2.2 Methods

Sand samples size distributions were conducted by the dry sieving methodology. The appropriate uniformity coefficient  $C_u$  and curvature coefficient  $C_c$  were determined based on the grain size distribution as follows:

$$C_u = \frac{D_{60}}{D_{10}} \quad (1)$$

$$C_c = \frac{D_{30}^2}{D_{60} * D_{10}} \quad (2)$$

$D_{10}$ ,  $D_{30}$ , and  $D_{60}$  [in  $\mu\text{m}$ ] are the grain diameters corresponding to 10 %, 30 %, and 60 % passing by weight, respectively. FTIR spectroscopy was used to investigate the structural characteristics of the powder sand samples in terms of bonding vibrations. Before the analysis, a pellet was formed by mixing 98 mg of KBr with 2 mg of sand powder and compressing the mixture with a die hydraulic press. Using a Shimadzu FTIR-8300 apparatus, the room temperature transmission infrared spectra were acquired within the wavenumber range 400-4000  $\text{cm}^{-1}$ . Furthermore, an X-ray fluorescence (XRF) spectrometer, type A Philips Cubix-XRF apparatus, was employed to assess the chemical composition of both powder sand samples. The mineralogical analyses were performed by an X-ray diffractometer (Bruker diffractometer) with a  $\lambda_{\text{CuK}\alpha 1} = 1.5406 \text{ \AA}$  and a scan step size of  $0.02^\circ$  over a  $2\theta$  range of  $5^\circ$  to  $90^\circ$ . Scanning electron microscope equipped with a dispersive energy X-ray (EDX) spectrometer type Phenom Pro Desktop SEM was utilized to examine the morphology and elemental composition of El-Baadj alluvial sand and dune sand samples.

### 3. Results and discussion

The photographs of the samples are illustrated in Figure 2. It is obvious that the size of the grains and color of the samples are significantly different.

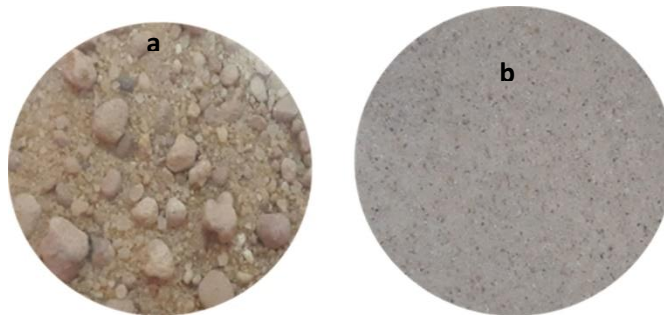


**Figure 2 - Photographs of (a) El-Baadj sand and (b) dune sand.**

#### 3.1 Physical Properties

The physical properties of the analyzed sand samples are summarized in Table 1. Aggregate specific gravity is commonly used as a criterion for their suitability as construction materials, and the lower the aggregate specific gravity, the more absorption and voids they contain (Abu Seif and Sonbul, 2019). The studied dune sand and El-Baadj sand showed a specific gravity ( $\rho_s$ ) of 2.58 and 2.60 ( $\text{g}/\text{cm}^3$ ), respectively, which completed the standard specifications (usually varying between 2.6 and 2.7) (Neville, 2011).

**Table 1 - Physical properties of El-Oued dune sand and El-Baadj sand.**

Properties	Dune sand	El-Baadj sand	Permissible limits	Ref.
Specific gravity / $\text{g}/\text{cm}^3$	2.58	2.60	2.60–2.70	(Neville, 2011)
Fineness modulus	1.16	2.91	2.30–3.20	(ASTM C33, 2003)
Bulk density / $\text{g}/\text{cm}^3$	1.49	1.65	1.30–1.75	(Mehta <i>et al.</i> , 2013)
Coefficient of uniformity	2.00	7.06	-	-
Coefficient of curvature	0.99	0.86	-	-
SE / %	84.0	72.01	-	-

The bulk density ( $\rho_{app}$ ) of El-Baadj sand was  $1.65 \text{ g/m}^3$  and of dune sand was  $1.49 \text{ g/m}^3$ , which is within the limits of  $1.30$  to  $1.75 \text{ g/m}^3$  required for typical weight concrete (Mehta *et al.*, 2013). El-Baadj sand has a higher bulk density than dune sand due to its lower void content. This means an inverse relationship between the bulk density and inter-aggregate void ratio (Al-Ansary *et al.*, 2013). However, the nature of the sand could be determined by measuring its sand equivalent (SE). The SE for dune sand was 72% and for El-Baadj sand was 84%. Therefore, the dune sand equivalent values suggested the existence of an insignificant amount of fine materials (clays and silts), which had been picked up by wind activity. El-Baadj sand, in contrast hand, has a significant proportion of fine materials. As a result, dune sand is classified as clean sand, suitable for high quality concrete (Guettouche *et al.*, 2023). Whereas El-Baadj sand is classified as clay sand.

### 3.2 Grading Analysis

The particle size distributions of the sand samples are given in Figure 3.

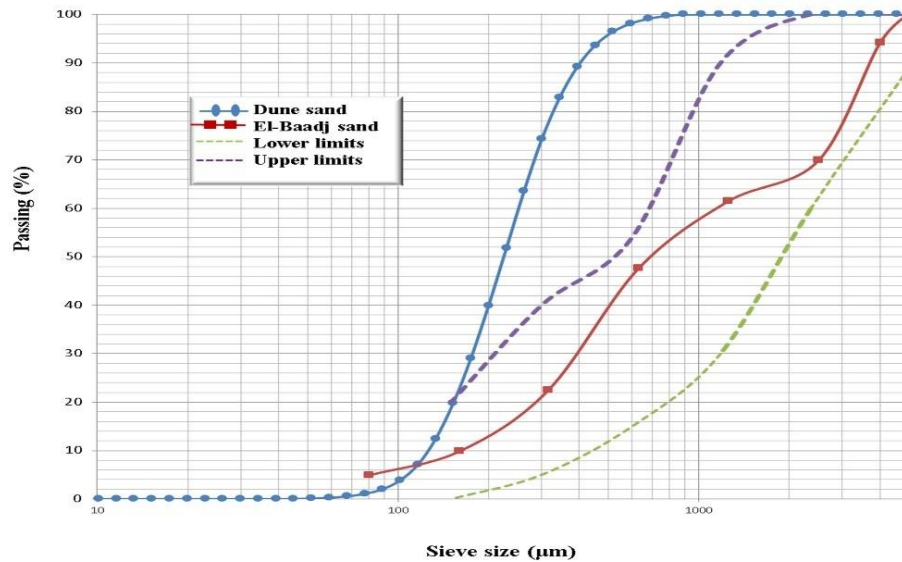


**Figure 3 - Granular curves of the dune sand and El-Baadj sand samples.**

El-Baadj alluvial sand presented a continuous particle size distribution ranging from 0 to 5 mm, while the dune sand had a more uniform gradation with more than 90 % of the grains smaller than 0.4 mm.

The grading curves of the El-Baadj sand fall within the upper and lower limits of the coarse grading limits (C) for fine aggregate specified by BS 882 (BS 882, 1992). However, the dune sand grading curve is outside the upper limit stipulated by BS 882. The fineness modulus (FM) value of dune sand was 1.16, and for alluvial sand was 2.95. Dune sand has a mean grain size of  $250 \mu\text{m}$ , indicating a fine sand grade, whereas Baadj alluvial sand has a mean grain size of  $406 \mu\text{m}$ , indicating a medium sand grade. According to the USCS classification system (Stevens *et al.*, 1982), the analyzed dune sand is classified as poorly graded sand ( $C_c < 1$ ,  $C_u < 6$ ), and El-Baadj sand is classified as well-graded sand ( $C_c < 3$ ,  $C_u > 6$ ). In reality, the fineness modulus and grain size distribution of the dune sand demonstrate that it does not meet the limitations for the fine aggregate gradations stipulated criteria. However, the fine aggregate for concrete is generally required to conform to any of the three grading limits of BS 882.

### 3.3 Fourier-Transform Infrared Analysis

Fourier-Transform Infrared (FTIR) spectroscopy is a powerful, efficient, and precise measurement tool for mineral analysis (Chandrasekaran *et al.*, 2021). The FTIR spectrum may be performed to determine the functional groups and consequently the components of sand samples. The FTIR spectra of El-Baadj alluvial sand and dune sand are displayed in Figure 4, as well as the Table 2 recapitulates the functional groups revealed in these sand samples. The IR spectra of the El-Baadj sand sample revealed significant peaks at 782 and 799  $\text{cm}^{-1}$ , which are assigned to the symmetric and asymmetric stretching vibration of the Si-O bond, respectively.

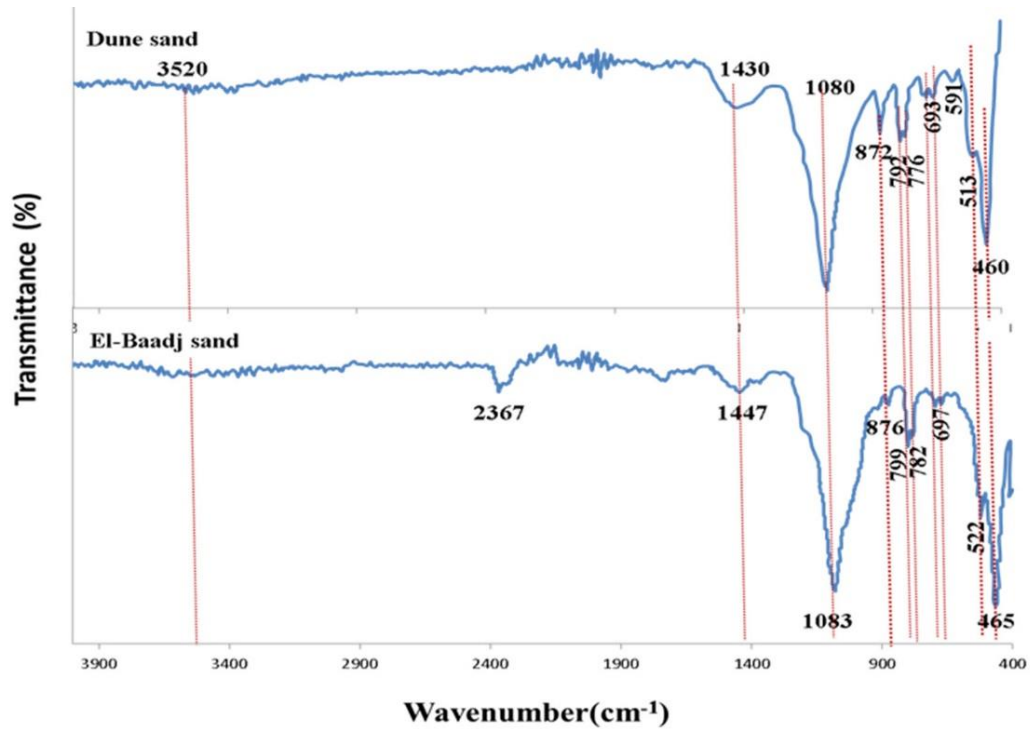


**Figure 4 - FTIR spectra of the El-Baadj sand and dune sand samples from El-Oued region.**

Moreover, the absorption bands that appear at 465 and 522  $\text{cm}^{-1}$  were attributed to the asymmetric bending vibration of the Si-O bond, and the 697 and 1083  $\text{cm}^{-1}$  were attributed to the symmetric vibration of the Si-O-Si bond. These functional groups affirmed that the  $\alpha$ -Quartz ( $\text{SiO}_2$ ) mineral was the main component of the El-Baadj sand. However, the absorption bands at 673  $\text{cm}^{-1}$  and 2363  $\text{cm}^{-1}$  represent the asymmetrical stretching vibration of  $(\text{SO}_4)^{2-}$ , which suggests the presence of gypsum ( $\text{CaSO}_4 \cdot 2\text{H}_2\text{O}$ ) in this sand. The absorption bands at 876  $\text{cm}^{-1}$ , 1447  $\text{cm}^{-1}$ , and 1763  $\text{cm}^{-1}$  refer to the asymmetrical stretching vibration of  $(\text{CO}_3)^{2-}$  and the C=O stretching mode vibration, respectively.

**Table 2 - The main bands of FTIR absorption and associated bond vibration of El-Baadj sand and dune sand from El-Oued region.**

Wave number / cm <sup>-1</sup>		Functional groups	Compounds	Ref.
Dune sand	El-baadj sand			
3520	3520	O–H stretching vibration	Water	(Benchaa <i>et al.</i> , 2021)
	2363	SO <sub>4</sub> <sup>-2</sup> asymmetrical stretching	Gypsum	(Anbalagan <i>et al.</i> , 2009)
/	1760	C=O stretching vibration	Calcite	(Kumar <i>et al.</i> 2014)
1430	1447	(CO <sub>3</sub> ) <sup>-2</sup> stretching vibration	Calcite	(Chandrasekaran <i>et al.</i> , 2021)
1080	1083	Si–O–Si symmetrical stretching	Quartz	(Meftah <i>et al.</i> , 2021)
872	876	(CO <sub>3</sub> ) <sup>-2</sup> out-of-plane bending	Calcite	(Meftah <i>et al.</i> , 2020)
792	799	Si–O asymmetrical stretching	Quartz	(Mechri <i>et al.</i> , 2017)
776	782	Si–O symmetrical stretching	Quartz	(Chen <i>et al.</i> , 2015; Naik <i>et al.</i> , 2021)
693	697	Si-O-Si symmetrical bending	Quartz	(Meftah <i>et al.</i> , 2020)
667	673	SO <sub>4</sub> <sup>-2</sup> asymmetrical stretching	Gypsum	(Liu <i>et al.</i> , 2018)
591	/	SO <sub>4</sub> <sup>-2</sup> asymmetrical stretching	Gypsum	(Benchaa <i>et al.</i> , 2021 ; Liu <i>et al.</i> , 2018)
513	522	Si-O-Si asymmetrical bending	Quartz	(Chandrasekaran <i>et al.</i> , 2021; Meftah <i>et al.</i> , 2020)
460	465	Si-O-Si asymmetrical bending	Quartz	(Mechri <i>et al.</i> , 2017)

The absorption band 3520 cm<sup>-1</sup> is induced by the asymmetric and symmetric stretching vibrations of H<sub>2</sub>O molecules in gypsum. These peaks suggested the presence of the calcite mineral. According to Kumar *et al.* (2014), the 1447 cm<sup>-1</sup> peak, within the range of 1400–1450 cm<sup>-1</sup>, suggests prevailing low pressure during the formation. Thus, all FTIR peaks reveal the existence of quartz, calcite, and gypsum in El-Baadj alluvial sand.

The FTIR spectra of “Zegoum” dune sand also revealed peaks at 776 cm<sup>-1</sup> and 793 cm<sup>-1</sup>, due to the Si-O bond's symmetric and asymmetric stretching vibration. The 459 cm<sup>-1</sup> and 513 cm<sup>-1</sup> absorption bands were also linked to the asymmetric bending vibration of the Si-O bond, and the absorption bands 693 cm<sup>-1</sup> and 1080 cm<sup>-1</sup> were assigned to the symmetric vibration of the Si-O-Si bond. These peaks prove the presence of  $\alpha$ -quartz in the dune sand. Other absorption peaks appeared at 1440 cm<sup>-1</sup> due to the C=O stretching mode vibration, indicating the presence of calcite mineral, as a carbonate mineral. In addition, an absorption band of 667 cm<sup>-1</sup> and 591 cm<sup>-1</sup> has been identified, which fits the asymmetrical stretching vibration of (SO<sub>4</sub>)<sup>-2</sup>. Therefore, these functional groups and demonstrate also that gypsum (CaSO<sub>4</sub>, 2H<sub>2</sub>O) is existing in dune sand.

### 3.4 Chemical Analysis

The chemical compositions of the sand samples were determined using XRF spectroscopy and are presented in Table 3. Silicon oxide (SiO<sub>2</sub>) is the most abundant component in the El-Baadj and dune sands, accounting for 80.9 and 70.8 %, respectively.

SiO<sub>2</sub> oxide represents the quartz mineral, a common component of natural sand, and it is the most common mineral and extensively distributed on the earth's surface (Meftah and Hani, 2022). However, the silicon oxide percentage in dune sand was more than that of El-Baadj sand. These results are consistent with the qualitative study of coarse fractions of Qatari sands (Al-Ansary and Iyengar, 2013). Moreover, the iron oxide proportion for El-Baadj and dune sand was 6.8 % and 5.5 %, respectively. We mention that the Fe<sub>2</sub>O<sub>3</sub> in El-Baadj sand is responsible for the reddish color of this sample (Muttashar *et al.*, 2018). The calcium oxide (CaO) content for the El-Baadj sand is

19.6 % and for the dune sand is 11 %. These oxides form calcite and gypsum minerals in the studied sample (Yaseen *et al.*, 2019). The alumina ( $\text{Al}_2\text{O}_3$ ) mass content for El-Baadj and dune sand was 1.25 % and 1.23 %, respectively. Both sand samples included low sulfur trioxide ( $\text{SO}_3$ ) concentrations, with 0.60 % in El-Baadj sand and 0.3 % in dune sand. MgO,  $\text{Na}_2\text{O}$ , and  $\text{K}_2\text{O}$  oxides were found in small amounts in both samples. These outcomes corroborate the dominance of quartz mineral in the El-Baadj alluvial and dune sand, with a minor amount of calcite. and trace content of  $\text{Fe}_2\text{O}_3$ ,  $\text{Al}_2\text{O}_3$ ,  $\text{Na}_2\text{O}$ ,  $\text{SO}_3$ , MgO,  $\text{TiO}_2$ ,  $\text{P}_2\text{O}_5$ , and  $\text{Mn}_3\text{O}_4$ .

**Table 3 - El-Baadj sand and dune sand chemical composition.**

Sample	El-Baadj sand	Dune sand
$\text{SiO}_2$ (%)	70.78	80.92
$\text{Al}_2\text{O}_3$ (%)	1.25	1.23
$\text{Fe}_2\text{O}_3$ (%)	6.81	5.47
CaO (%)	19.56	11.02
MgO (%)	0.42	0.33
$\text{K}_2\text{O}$ (%)	0.30	0.40
$\text{Na}_2\text{O}$ (%)	0.100	0.103
$\text{SO}_3$ (%)	0.60	0.30
Cl (%)	0.013	0.012
$\text{P}_2\text{O}_5$ (%)	0.045	0.039
$\text{TiO}_2$ (%)	0.112	0.096
$\text{Mn}_3\text{O}_4$ (%)	0.038	0.036

### 3.5 XRD Analysis

To determine the different mineral phases, present in sand samples, the XRD method was employed. Figure 5 depicts the XRD patterns of alluvial sand and dune sand. Minerals were identified using the computer program X'Pert High Score and PDF cards. The alluvial sand showed diffraction peaks at  $2\theta$ :  $20.89^\circ$ ,  $26.66^\circ$ ,  $36.56^\circ$ ,  $39.46^\circ$ ,  $40.31^\circ$ ,  $42.47^\circ$ ,  $45.80^\circ$ ,  $50.16^\circ$ ,  $54.87^\circ$ ,  $59.97^\circ$ ,  $67.75^\circ$ ,  $68.16^\circ$ ,  $68.34^\circ$ , and  $81.50^\circ$  that corresponding respectively to the crystalline planes (100), (101), (210), (102), (111), (200), (201), (112), (003), (211), (212), (203), (301) and (310). According to the JCPDS (N<sup>o</sup> 00-046-1045), these XRD peaks are assigned to the  $\alpha$ -quartz phase ( $\text{SiO}_2$ ), which has a hexagonal crystalline structure and is assigned to the space group  $\text{P3}_221$  (154) (Hassan *et al.*, 2017). However, the peaks observed at  $2\theta$ :  $23.1^\circ$ ,  $29.42^\circ$ ,  $36.01^\circ$ ,  $47.53^\circ$ , and  $48.54^\circ$  corresponded to the crystalline planes (012), (104), (110), (018), and (116), respectively. According to the JCPDS (N<sup>o</sup> 01-086-2344), these results indicate the presence of calcite mineral ( $\text{CaCO}_3$ ) with a trigonal crystalline structure and belonging to the space group R-3c (167) (Oglesbee *et al.*, 2020). Moreover, diffraction peaks (crystalline planes) at  $11.65^\circ$ (020),  $20.87^\circ$ (-121),  $36.56^\circ$ (-222),  $39.46^\circ$ (-161), and  $43.19^\circ$ (240) are induced by gypsum ( $\text{CaSO}_4 \cdot 2\text{H}_2\text{O}$ ) with a monoclinic crystal system and the space group I2/c, according to the JCPDS (No 01-074-1905) (Hadjadj *et al.*, 2020).

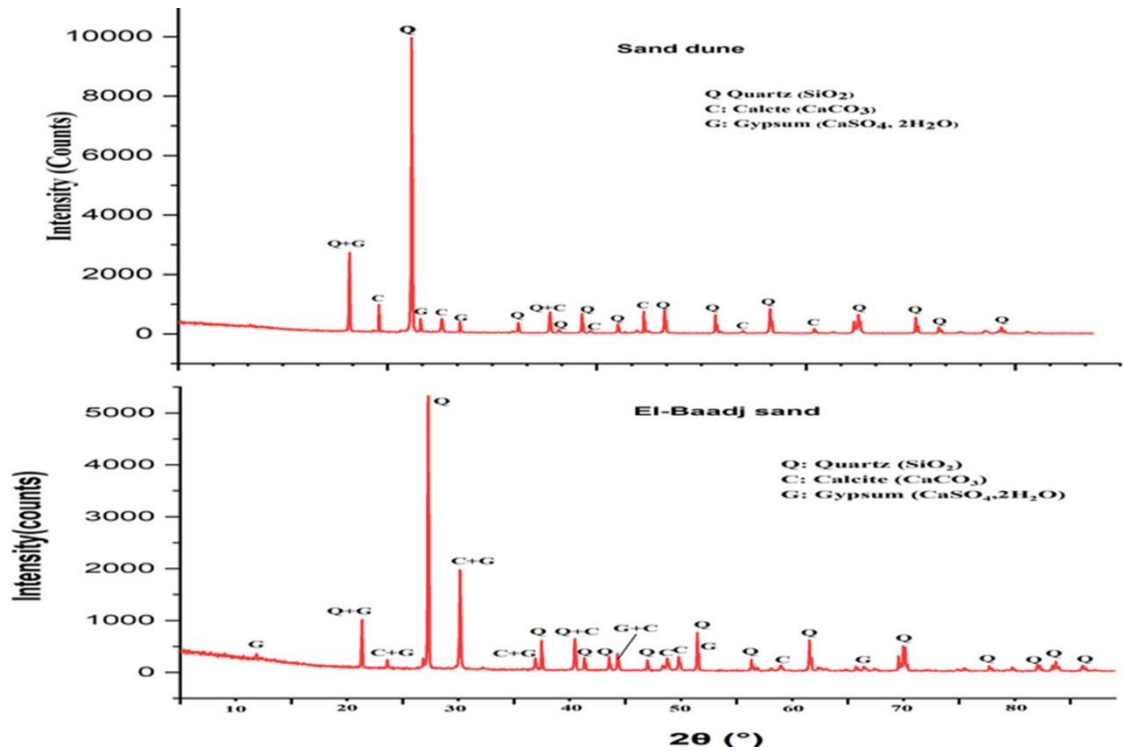


**Figure 5 - XRD patterns of the El-Baadj and dune sand from El-Oued region.**

These findings indicate that the El-Baadj sand consists mainly of  $\alpha$ -quartz, calcite, and gypsum minerals, which are in conformity with the results found by Al-Ansary *et al.* on the Qatar fluvial sand (Al-Ansary and Iyengar, 2013).

However, the XRD patterns of the Zegoum dune sand show peaks at  $2\theta$ : 20.88°, 26.64°, 36.55°, 39.46°, 42.47°, 50.16°, 54.87°, 59.97°, 64.1°, 67.75°, 68.16°, 68.34°, 73.32°, 75.72°, and 81.49°, according to the JCPDS (N° 00-046-1045) corresponding to the (hkl) crystalline planes (100), (101), (210), (102), (111), (201), (112), (003), (211), (113), (212), (203), (301), (104), (302), and (310), respectively. These crystalline planes also support the occurrence of the  $\alpha$ -quartz phase (SiO<sub>2</sub>) in the dune sand sample, which has a hexagonal crystalline structure and belongs to the P3<sub>2</sub>21 space group (154) (Meftah *et al.*, 2020).

Furthermore, the JCPDS card (N° 01-086-2334) confirms that the four significant reflections at  $2\theta$ : 23.09°, 29.42°, 39.46°, 43.19°, and 48.54°, corresponding respectively to the (hkl) crystalline planes (012), (104), (113), (202), and (116), represent calcite minerals (Benchara *et al.*, 2021). The gypsum diffraction peaks were recorded at 20.87°, 27.48°, and 31.16°, with (220), (041), and (022) crystalline planes, according to the JCPDS card (N° 01-076-1746). The dune sand sample contains monoclinic gypsum (CaSO<sub>4</sub>·2H<sub>2</sub>O) that belongs to the space group C2/m.

The XRD semi quantification of these minerals is illustrated in the Table 4. Both El-Baadj alluvial sand and dune sand are mainly composed of  $\alpha$ -Quartz crystalline minerals, with minor amounts of calcite and a very low amount of gypsum minerals. The dune sand has a higher ratio of quartz (about 73 % SiO<sub>2</sub>) than the El-Baadj sand (about 70 % SiO<sub>2</sub>), while the El-Baadj sand has a higher ratio of gypsum and calcite by 5 % CaSO<sub>4</sub>·2H<sub>2</sub>O and 25 % CaCO<sub>3</sub>, respectively.

The quartz mineral is commonly known to be nonreactive (Muttashar *et al.*, 2018), but generally improves the packing density and long-term strength development.

**Table 4 - Semi-quantitative analysis of El-Baadj and dune sands.**

Mineral	Chemical formula	Relative % composition	
		Dune sand	El-Baadj sand
Quartz	SiO <sub>2</sub>	73.0	70.3
Calcite	CaCO <sub>3</sub>	23.0	24.7
Gypsum	CaSO <sub>4</sub> ·2H <sub>2</sub> O	4.0	5.0

It may be beneficial for forming calcium silicate hydrate gel or calcium aluminum silicate hydrate in concrete (Muttashar *et al.*, 2018). On the other hand, calcite produces an adhesive scale on most metals, which reduces corrosion. The obtained XRD results are in good accordance with FT-IR and XRF analysis, which indicated the existence of quartz, calcite, and gypsum minerals in both samples. As well, the quartz crystalline mineral is considered a major component in the El-Baadj and dune sand samples.

### 3.6 SEM–EDS Analysis

The fine aggregate particles' size and shape significantly impact the strength, durability, and workability of hardened mixtures (Abu Seif, 2019). Further, the well-graded angular grains have better packing strength and durability in hardened mixtures (El-Shater *et al.*, 2020). However, SEM/EDX investigations are beneficial for determining sample surface structure and morphology and the superficial elemental profile. The surface and grain morphology of El-Baadj sand and dune sand samples were studied using the backscattered scanning electron microscope (BSE) mode. As indicated in Figure (6-a), the grain size of El-Baadj sand samples varies from medium to coarse sand, which is in agreement with the particle size distribution outcomes given in Figure 2. In addition, the grains are poorly sorted and appear in a variety of shapes and sizes, ranging from angular to well-rounded, where argillaceous and clayey fines appear to cover the surface. The Figure (6-b) exhibits the surface micrograph of the studied dune sand.

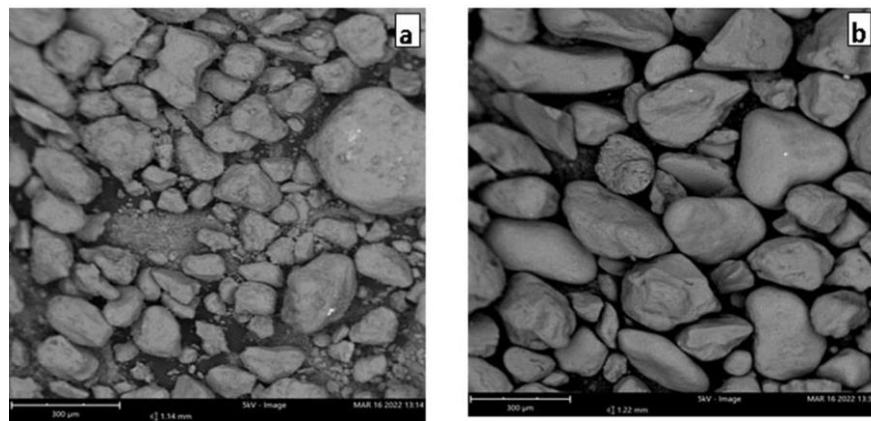


**Figure 6 - SEM surface micrograph (a) El-Baadj construction sand and (b) dune sand.**

The dune sand is well sorted, with sub-angular to well-rounded grains and a single uniform size. However, they are generally more rounded because air-transported grains are intensively subjected to pitting and become round faster than those transported in aqueous media (Seif 2013). This sand appears to be clean and free of fines.

The energy-dispersive X-ray spectroscopy (EDX) analysis of El-Baadj sand and dune sand samples are shown in Figure 7. EDS results display that silicon (Si) and oxygen (O) elements are the significant components across both samples and are most dominant in the dune sand sample.

We notice that silica ( $\text{SiO}_2$ ) is the predominant mineral in the investigated samples as seen in Figure 7. The calcium (Ca) element is the third dominant element in the studied sand samples.

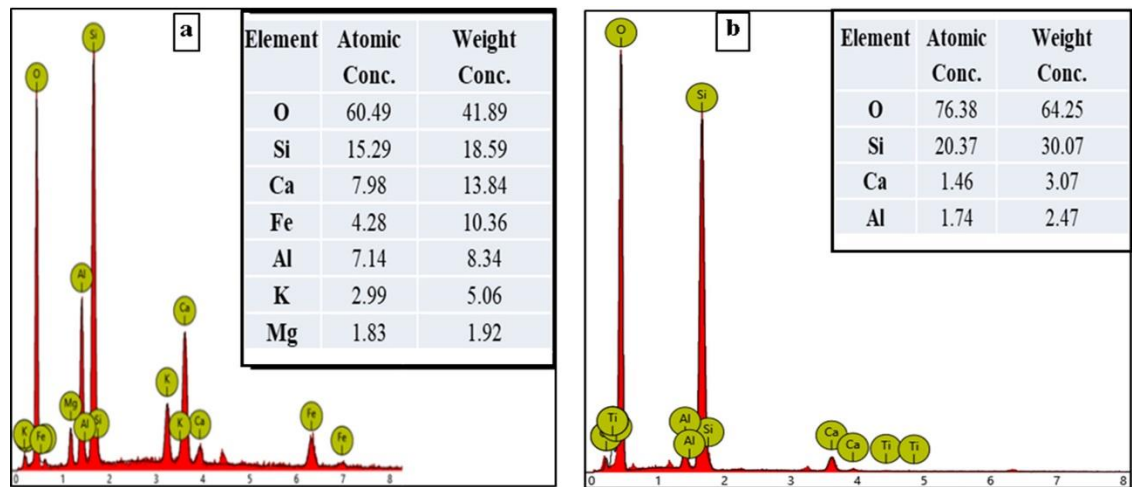


**Figure 7 - Energy-dispersive X-ray spectroscopy analysis of (a) El-Baadj sand and (b) dune sand samples.**

The EDX spectra also showed the presence of an aluminum element (Al) in the El-Baadj and dune sand samples. Other minor elements, such as iron (Fe), potassium (K), and magnesium (Mg), were only found in the El-Baadj sand samples. Overall, these elemental compositions confirm the XRF chemical analysis accomplished in section 3.4. Thus, the examined sands: El-Baadj alluvial and dune sands were mineralogically stable and chemically appropriate for use as fine aggregates in concrete and cement mortar.

#### 4. Conclusion

This research presents, for the first time, a comprehensive and scientific comparison of dune sand and El-Baadj alluvial sand from the El-Oued province (Northeast Algerian Sahara) regarding their physical, microstructural, and chemical characteristics to prove their utility in construction applications. The El-Baadj alluvial sand was found to be medium sand, well-graded, and its physical properties meet the standard specification limits. Consequently, El-Baadj alluvial sands are appropriate for utilization as construction aggregates. However, the Zegoum dune sand was determined to be fine sand with poor grading. Some of its physical parameters (i.e., fineness modulus and bulk density) did not meet the standards' specifications. Thus, the dune sands need to improve their poor gradation to be suitable for constructing fine aggregates. According to the FTIR results, most functional groups in El-Baadj and dune sand represent quartz minerals, and some vibration bonds represent calcite and gypsum minerals. The chemical analysis by XRF revealed that the dune sand has a silica content (80 %  $\text{SiO}_2$ ) higher than El-Baadj sand (70 %  $\text{SiO}_2$ ). Calcium oxide ( $\text{CaO}$ ), iron oxide ( $\text{Fe}_2\text{O}_3$ ), and sulfur trioxide ( $\text{SO}_3$ ) were higher in El-Baadj sand. Furthermore, the XRD analysis confirmed that  $\alpha$ -quartz ( $\text{SiO}_2$ ) was the predominant compound in dune sand and El-Baadj sand samples, whereas calcite ( $\text{CaCO}_3$ ) and gypsum ( $\text{CaSO}_4 \cdot 2\text{H}_2\text{O}$ ) minerals were found in lower amounts in both sands. The grain size of El-Baadj sand samples ranges from medium to coarse sand and is angular to well-rounded. In contrast, the Zegoum dune sand is well-sorted, with subangular to well-rounded grains. These findings state that El-Baadj alluvial sand and dune sand are suitable for construction applications, except the latter needs some improvement in their poor gradation.

## References

- Abdelhak, M., Ahmed, K., Abdelkader, B., Brahim, Z., & Rachid, K. (2014). Algerian sahara sand dunes characterization. *Silicon*, 6, 149-154. <https://doi.org/10.1007/s12633-014-9196-0>
- Abu Seif, E. S. S. (2015). Geotechnical approach to evaluate natural fine aggregates concrete strength, Sohag, Governorate, Upper Egypt. *Arabian Journal of Geosciences*, 8(9), 7565-7575. <https://doi.org/10.1007/s12517-014-1705-3>
- Abu Seif, E. S. S., & Sonbul, A. R. (2019). Geotechnical performance of sandy bricks made with fine aggregates of sand dunes, Saudi Arabia. *Arabian Journal of Geosciences*, 12, 1-14. <https://doi.org/10.1007/s12517-019-4345-9>
- Al-Ansary, M., & Iyengar, S. R. (2013). Physiochemical characterization of coarse aggregates in Qatar for construction industry. *International Journal of Sustainable Built Environment*, 2(1), 27-40.
- Amri, S., Akchiche, M., Bennabi, A., & Hamzaoui, R. (2019). Geotechnical and mineralogical properties of treated clayey soil with dune sand. *Journal of African Earth Sciences*, 152, 140-150. <https://doi.org/10.1016/j.jafrearsci.2019.01.010>
- Anbalagan, G., Mukundakumari, S., Murugesan, K. S., & Gunasekaran, S. (2009). Infrared, optical absorption, and EPR spectroscopic studies on natural gypsum. *Vibrational Spectroscopy*, 50(2), 226-230. <https://doi.org/10.1016/j.vibspec.2008.12.004>
- ASTM C33. (2003). *American standard testing of materials-specification for concrete aggregates*, American society of testing and materials Publication, pp.11.
- Ayyam, V., Palanivel, S., & Chandrakasan, S. (2019). *Coastal ecosystems of the Tropics-adaptive management*. Springer Singapore.
- Barkat, A., Bouaicha, F., Bouteraa, O., Mester, T., Ata, B., Balla, D., and Szabó, G. (2021). Assessment of complex terminal groundwater aquifer for different use of Oued Souf valley (Algeria) using multivariate statistical methods, geostatistical modeling, and water quality index. *Water*, 13(11), 1609. <https://doi.org/10.3390/w13111609>
- Benchaa, S., Gheriani, R., Achouri, A., Bouguettaia, H., & Mechri, M. L. (2021). Structural characterizations of dune sand and construction sand of Sidi Slimane and Zaouia El Abidia areas in the Touggourt region in southeast Algeria. *Arabian Journal of Geosciences*, 14, 1-11. <https://doi.org/10.1007/s12517-021-08303-9>
- BS 882. (1992). *Specification for Aggregate from Natural Sources for Concrete 14 BSI Standards Publication*.
- Chandrasekaran, A., Senthil Kumar, C. K., Sathish, V., Manigandan, S., & Tamilarasi, A. (2021). Effect of minerals and heavy metals in sand samples of Ponnai river, Tamil Nadu, India. *Scientific Reports*, 11(1), 23199. <https://doi.org/10.1038/s41598-021-02717-x>
- Chen, Y., Zou, C., Mastalerz, M., Hu, S., Gasaway, C., & Tao, X. (2015). Applications of micro-fourier transform infrared spectroscopy (FTIR) in the geological sciences—a review. *International journal of molecular sciences*, 16(12), 30223-30250. <https://doi.org/10.3390/ijms161226227>
- Elipe, M. G., & López-Querol, S. (2014). Aeolian sands: Characterization, options of improvement and possible employment in construction—The State-of-the-art. *Construction and Building Materials*, 73, 728-739. <https://doi.org/10.1016/j.conbuildmat.2014.10.008>
- El-Shater, A. A. H., Mahran, T. M., Abu Seif, E. S. S., & Mahmoud, K. (2020). Geotechnical study on the utilization of Pleistocene Sands in Sohag Basin (Upper Egypt) as a construction raw material. *Environmental Earth Sciences*, 79, 1-20. <https://doi.org/10.1007/s12665-020-09302-x>
- Fontaine J. (2005). In *Annales de géographie*. Armand Colin, 4, 437-448.
- Ganesan, K., Kanagarajan, V., & Dominic, J. R. J. (2022). Influence of marine sand as fine aggregate on mechanical and durability properties of cement mortar and concrete. *Materials Research Express*, 9(3), 035504. <https://doi.org/10.1088/2053-1591/ac5f88>
- Gourley, J. J., & Calvert, C. M. (2003). Automated detection of the bright band using WSR-88D data. *Weather and Forecasting*, 18(4), 585-599. <https://doi.org/10.1175/1520-0434>

- Guettouche, A., Merdas, A., Berrabah, F., & Guechi, L. (2023, April). Valorization of Cement Kiln Dust (CKD) from the Ain-Al-Kebira Cement Plant (Algeria) in Building Materials. *In Annales de Chimie Science des Matériaux* 47(2). <https://doi.org/10.18280/acsm.470201>
- Hadjadj, K., & Chihi, S. (2020). Rietveld refinement based quantitative phase analysis (QPA) of Ouargla (part of Grand Erg Oriental in Algeria) dunes sand. *Silicon*, 1-9. <https://doi.org/10.1007/s12633-020-00826-2>
- Hassan, W. N. F. W., Ismail, M. A., Lee, H., Hussin, M. W., Ismail, M., & Singh, J. K. (2017). Utilization of nano agricultural waste to improve the workability and early strength of concrete. *International Journal of Sustainable Building Technology and Urban Development*, 8(4), 316-331.
- Kirthika, S. K., Singh, S. K., & Chourasia, A. (2020). Alternative fine aggregates in production of sustainable concrete-A review. *Journal of cleaner production*, 268, 122089. <https://doi.org/10.1016/j.jclepro.2020.122089>
- Kumar, R. S., & Rajkumar, P. (2014). Characterization of minerals in air dust particles in the state of Tamilnadu, India through FTIR, XRD and SEM analyses. *Infrared Physics & Technology*, 67, 30-41. <https://doi.org/10.1016/j.infrared.2014.06.002>
- Lai, X., Shankman, D., Huber, C., Yesou, H., Huang, Q., & Jiang, J. (2014). Sand mining and increasing Poyang Lake's discharge ability: A reassessment of causes for lake decline in China. *Journal of Hydrology*, 519, 1698-1706. <https://doi.org/10.1016/j.jhydrol.2014.09.058>
- Liu, Y. (2018). Raman, Mid-IR, and NIR spectroscopic study of calcium sulfates and mapping gypsum abundances in Columbus Crater, Mars. *Planetary and Space Science*, 163, 35-41. <https://doi.org/10.1016/j.pss.2018.04.010>
- Lollini, F., Carsana, M., & Bertolini, L. (2017). A study on the cement-based decorative materials in the San Fedele Church in Milan. *Case studies in construction materials*, 7, 36-44. <https://doi.org/10.1016/j.cscm.2017.05.004>
- Lopez-Querol, S., Arias-Trujillo, J., Maria, G. E., Matias-Sanchez, A., & Cantero, B. (2017). Improvement of the bearing capacity of confined and unconfined cement-stabilized aeolian sand. *Construction and Building Materials*, 153, 374-384. <https://doi.org/10.1016/j.conbuildmat.2017.07.124>
- Luo, F. J., He, L., Pan, Z., Duan, W. H., Zhao, X. L., & Collins, F. (2013). Effect of very fine particles on workability and strength of concrete made with dune sand. *Construction and Building Materials*, 47, 131-137. <https://doi.org/10.1016/j.conbuildmat.2013.05.005>
- Mechri, M. L., Chihi, S., Mahdadi, N., & Beddiaf, S. (2017). Diagnosis of the heating effect on the electrical resistivity of Ouargla (Algeria) dunes sand using XRD patterns and FTIR spectra. *Journal of African Earth Sciences*, 125, 18-26. <https://doi.org/10.1016/j.jafrearsci.2016.10.007>
- Meftah, N., & Mahboub, M. S. (2020). Spectroscopic characterizations of sand dunes minerals of El-Oued (Northeast Algerian Sahara) by FTIR, XRF and XRD analyses. *Silicon*, 12(1), 147-153. <https://doi.org/10.1007/s12633-019-00109-5>
- Meftah, N., Hani, A., Merdas, A., Sadik, C., & Sdiri, A. (2021). A holistic approach towards characterizing the El-Oued siliceous sand (eastern Algeria) for potential industrial applications. *Arabian Journal of Geosciences*, 14, 1-14. <https://doi.org/10.1007/s12517-021-08591-1>
- Meftah, N., and Hani, A. (2022). Characterization of Algerian dune sand as a source to metallurgical-grade silicon production. *Materials Today: Proceedings*, 51, 2105-2108. <https://doi.org/10.1016/j.matpr.2021.12.366>
- Mehta P.K., and Monteiro P. J. M. (2013). *Concrete: Microstructure, Properties, and Materials*. McGraw-Hill Education. <https://doi.org/10.1016/j.ijsbe.2013.07.003>
- Moulay-Ali, A., Abdeldjalil, M., & Khelafi, H. (2021). An experimental study on the optimal compositions of ordinary concrete based on corrected dune sand—Case of granular range of 25 mm. *Case Studies in Construction Materials*, 14, e00521.
- Muttashar, H. L., Ali, N. B., Ariffin, M. A. M., & Hussin, M. W. (2018). Microstructures and physical properties of waste garnets as a promising construction materials. *Case studies in*

- construction materials*, 8, 87-96. <https://doi.org/10.1016/j.cscm.2017.12.001>.
- Naik, A. S., Behera, B., Shukla, U. K., Sahu, H. B., Singh, P. K., Mohanty, D., ... & Chatterjee, D. (2021). Mineralogical studies of Mahanadi basin coals based on FTIR, XRD and microscopy: a geological perspective. *Journal of the Geological Society of India*, 97, 1019-1027. <https://doi.org/10.1007/s12594-021-1817-9>
- Neville A. M. (2011). *Properties of Concrete*, Pearson Education Limited, London.
- Oglesbee, T., McLeod, C. L., Chappell, C., Vest, J., Sturmer, D., & Krekeler, M. P. (2020). A mineralogical and geochemical investigation of modern aeolian sands near Tonopah, Nevada: Sources and environmental implications. *Catena*, 194, 104640. <https://doi.org/10.1016/j.catena.2020.104640>
- Seif, E. S. S. A. (2013). Assessing the engineering properties of concrete made with fine dune sands: an experimental study. *Arabian Journal of Geosciences*, 6, 857-863. <https://doi.org/10.1007/s12517-011-0376-6>
- Smaida, A., Haddadi, S., & Nechnech, A. (2019). Improvement of the mechanical performance of dune sand for using in flexible pavements. *Construction and Building Materials*, 208, 464-471. <https://doi.org/10.1016/j.conbuildmat.2019.03.041>
- Stevens, J. (1982). Unified soil classification system. *Civil Engineering—ASCE*, 52(12), 61-62.28
- Yaseen, S. A., Yiseen, G. A., & Li, Z. (2019). Elucidation of calcite structure of calcium carbonate formation based on hydrated cement mixed with graphene oxide and reduced graphene oxide. *ACS omega*, 4(6), 10160-10170. <https://doi.org/10.1021/acsomega.9b00042>.
- Zhang, C., Li, Z., Chen, Q., Dong, S., Yu, X., & Yu, Q. (2020). Provenance of eolian sands in the Ulan Buh Desert, northwestern China, revealed by heavy mineral assemblages. *Catena*, 193, 104624. <https://doi.org/10.1016/j.catena.2020.104624>